

Unconventional superconductivity in $\text{YNi}_2\text{B}_2\text{C}$

This article has been downloaded from IOPscience. Please scroll down to see the full text article.

2009 J. Phys.: Condens. Matter 21 415704

(<http://iopscience.iop.org/0953-8984/21/41/415704>)

View [the table of contents for this issue](#), or go to the [journal homepage](#) for more

Download details:

IP Address: 129.252.86.83

The article was downloaded on 30/05/2010 at 05:34

Please note that [terms and conditions apply](#).

Unconventional superconductivity in $\text{YNi}_2\text{B}_2\text{C}$

T R Abu Alrub¹ and S H Curnoe

Department of Physics and Physical Oceanography, Memorial University of Newfoundland,
St John's, NL, A1B 3X7, Canada

Received 2 June 2009, in final form 23 July 2009

Published 23 September 2009

Online at stacks.iop.org/JPhysCM/21/415704

Abstract

We use the semiclassical (Doppler shift) approximation to calculate magnetic field angle-dependent density of states and thermal conductivity κ_{zz} for a superconductor with a quasi-two-dimensional Fermi surface and line nodes along $k_x = 0$ and $k_y = 0$. The results are shown to be in good quantitative agreement with experimental results obtained for $\text{YNi}_2\text{B}_2\text{C}$ (Izawa K *et al* 2002 *Phys. Rev. Lett.* **89** 137006).

1. Introduction

$\text{YNi}_2\text{B}_2\text{C}$ is a type II superconductor with a relatively high transition temperature $T_c = 15.6$ K [2]. Although initially thought to be a conventional s-wave superconductor, accumulated evidence soon suggested otherwise. Power law behaviour in the heat capacity $C_p/T \propto T^2$ was the first indication that $\text{YNi}_2\text{B}_2\text{C}$ is an unconventional superconductor with point nodes in the gap function [3, 4]. However, the field dependence of the heat capacity and thermal conductivity was found to be $C_p \propto \sqrt{H}$, indicative of line nodes [1, 4, 5]. The NMR spin relaxation rate $1/T_1$ was measured to be $\propto T^3$ with no Hebel–Slichter peak [6], again consistent with line nodes in the gap function. Finally, Raman scattering showed a peak in the electronic A_{1g} and B_{2g} response [7], possibly indicative of a B_{2g} symmetry gap function. Such a gap function takes the form $\Delta(\mathbf{k}) \propto k_x k_y$ and thus has symmetry-required line nodes along $k_x = 0$ and $k_y = 0$ [8, 9]. In contrast to these findings, field-angle-dependent measurements of thermal conductivity and specific heat were claimed to be indicative of point nodes in the gap function [1, 10, 11]. The reconciliation of these results, and hence the symmetry of the gap function, remains an important unresolved issue.

$\text{YNi}_2\text{B}_2\text{C}$ belongs to the crystallographic space group $I4/mmm$ (No. 139, D_{4h}^{17}) [12]. The lattice is body-centred tetragonal (bct) with $a = 3.526$ Å and $c = 10.543$ Å [3]. According to symmetry analysis for D_{4h} crystals [8, 9], gap functions with line nodes are found only for singlet pairing, while point nodes are found only for triplet pairing. Various nodal configurations can occur, depending on the irreducible representation of D_{4h} by which the superconducting order

parameter transforms. Nodes in the gap function are normally detected via quasiparticles (qps) which appear in the vicinity of gap nodes in k -space as a result of either finite temperature, impurities or Doppler shift in the presence of an applied magnetic field. In these kinds of measurements, the nodes will be invisible if there is no Fermi surface in the direction of the nodes; thus the shape and connectivity of the Fermi surface plays an important role.

The Fermi level crosses the 17th, 18th and 19th bands. The topology of the Fermi surface is highly sensitive to the precise position of the Fermi level due to a dispersionless band between the Γ and X points. Thus different band structure calculations share common features but the resulting Fermi surfaces have significant differences [13–15]. Yamaguchi *et al* [15] correlated their results with de Haas–van Alphen (dHvA) measurements in order to fix the Fermi energy. The 18th and 19th bands were found to produce closed Fermi surfaces around various points in the Brillouin zone. However, the 17th band produces a large electron Fermi surface multiply connected by necks. Part of this surface appears as dHvA oscillations perpendicular to the c axis. The orbits do not appear to be closed in the c direction; instead, they seem to possess a two-dimensional character that extends in the c direction, as shown by the upward curvature of the dHvA frequencies about the [001] direction, shown in figure 3 of [15].

In the vortex phase of a type II superconductor qps may be either *localized* about vortex cores or *delocalized*. It was shown some time ago that the contribution to the low-energy density of states in a superconductor with line nodes comes from *delocalized qps in the vicinity of the nodes* [16]. The delocalized qps can be treated with a semiclassical (Doppler shift) approximation; this approach provided a good description of field-angle-dependent specific heat and thermal conductivity of the line node

¹ Present address: Department of Physics, King Fahd University of Petroleum and Minerals, PO Box 785, Dhahran 31261, Saudi Arabia.

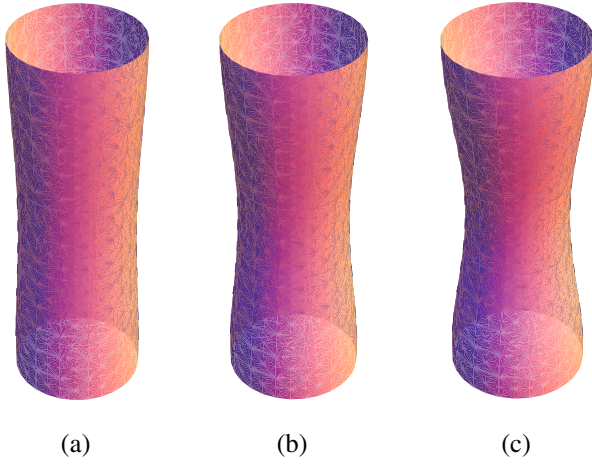


Figure 1. Fermi surfaces for three different values of $b = \frac{v'_c}{v_F}$. The surface in (c) has the largest value of b . (This figure is in colour only in the electronic version)

superconductors $\text{YBa}_2\text{Cu}_3\text{O}$ [17, 18] and CeCoIn_5 [19]. However, Volovik's argument does not extend to typical point node superconductors for which the gap function vanishes *linearly* in k . For these point node superconductors, the semiclassical calculation may still be performed [20] but, as may be expected, these results are not in agreement with any experiment involving putative point node superconductors so far.

In this paper, we use the semiclassical approximation to calculate the field-angle-dependent density of states and thermal conductivity for a superconductor with line nodes and a quasi-2D Fermi surface, for the purpose of demonstrating that the results of such measurements on $\text{YNi}_2\text{B}_2\text{C}$ are, in fact, consistent with this scenario, in contrast to what has been claimed [1].

For simplicity, we assume that the Fermi surface has the shape shown in figure 1, for which the qp energy spectrum takes the form

$$\varepsilon(\mathbf{k}) = \frac{k_x^2 + k_y^2}{2m} + \varepsilon'_F \cos ck_z - \varepsilon_F \quad (1)$$

where $\varepsilon'_F \equiv \frac{k'_c c^{-1}}{2m} \ll \varepsilon_F$. A gap function with B_{2g} symmetry has line nodes along $k_x = 0$ and $k_y = 0$. The Fermi momenta along these nodes (parametrized by k_z) are

$$\mathbf{k}_{F1,3} = (0, \pm(2m(\varepsilon_F - \varepsilon'_F \cos ck_z))^{1/2}, k'_F \sin ck_z) \approx (0, \pm k_F, k'_F \sin ck_z) \quad (2)$$

$$\mathbf{k}_{F2,4} = (\pm(2m(\varepsilon_F - \varepsilon'_F \cos ck_z))^{1/2}, 0, k'_F \sin ck_z) \approx (\pm k_F, 0, k'_F \sin ck_z). \quad (3)$$

The magnetic field rotates in the xy plane with an angle ϵ with respect to the x axis:

$$\mathbf{H} = H(\cos \epsilon, \sin \epsilon, 0). \quad (4)$$

The supercurrent circulates perpendicular to the field as a function of the distance r from the vortex core and winding angle β :

$$\mathbf{v}_s(\mathbf{r}) = \frac{1}{2mr} (-\sin \epsilon \cos \beta, \cos \epsilon \cos \beta, \sin \beta). \quad (5)$$

The Doppler shifts associated with each line node are $\alpha_i(\mathbf{r}) = \mathbf{k}_{Fi} \cdot \mathbf{v}_s$:

$$\alpha_{1,3}(\mathbf{r}) = \frac{1}{2mr} [\pm k_F \cos \epsilon \cos \beta + k'_F \sin \beta \sin ck_z] \quad (6)$$

$$\alpha_{2,4}(\mathbf{r}) = \frac{1}{2mr} [\mp k_F \sin \epsilon \cos \beta + k'_F \sin \beta \sin ck_z]. \quad (7)$$

2. Density of states

In the semiclassical treatment, the argument of Green's function $i\omega_n$ is replaced by $i\omega_n + \alpha$, where α is the Doppler shift. The quasiparticle energy is $E(\mathbf{k}) = \sqrt{\varepsilon^2(\mathbf{k}) + \Delta^2(\mathbf{k})}$, which is $\approx \sqrt{v_F^2 k_1^2 + v_g^2 k_2^2}$ in the vicinity of a node [23]. Here k_1 points in the direction of the node, k_2 is perpendicular to k_1 in the xy plane and the gap velocity is $v_g = \partial \Delta / \partial k_2|_{\text{node}}$. In the vicinity of the j th node, Green's function takes the form

$$G(\mathbf{k}, i\tilde{\omega}_n, \mathbf{r}) = \frac{i\tilde{\omega}_n + \alpha_j(\mathbf{r}) + v_F k_1}{(i\tilde{\omega}_n + \alpha_j(\mathbf{r}))^2 + v_F^2 k_1^2 + v_g^2 k_2^2} \quad (8)$$

where $i\tilde{\omega}_n = i\omega_n + i\Gamma_0$ and Γ_0 is the scattering rate at zero energy. The density of states is

$$N(\omega, \mathbf{r}) = -\frac{1}{\pi} \sum_{\mathbf{k}} \text{Im} G(\mathbf{k}, \tilde{\omega}, \mathbf{r}). \quad (9)$$

We divide the volume of integration into four curved cylinder-shaped volumes, each centred around a line node on the Fermi surface [23], and perform the integration across the disc spanned by k_1 and k_2 :

$$N(0, \mathbf{r}) = \frac{\Gamma_0}{4\pi^3 v_F v_g} \sum_{j=1}^4 \int_{-\pi/c}^{\pi/c} dk_z \times \left[\ln \frac{p_0}{\sqrt{\alpha_j^2(\mathbf{r}) + \Gamma_0^2}} + \frac{\alpha_j(\mathbf{r})}{\Gamma_0} \tan^{-1} \frac{\alpha_j(\mathbf{r})}{\Gamma_0} \right] \quad (10)$$

where p_0 is the integration cutoff. In the clean limit $|\alpha_j / \Gamma_0| \gg 1$ the density of states is

$$N(0, \mathbf{r}) = \frac{1}{4\pi^3 v_F v_g} \int_{-\pi/c}^{\pi/c} dk_z (|\alpha_1(\mathbf{r})| + |\alpha_2(\mathbf{r})| + |\alpha_3(\mathbf{r})| + |\alpha_4(\mathbf{r})|). \quad (11)$$

Averaging over the vortex cross section, we obtain

$$\langle N(0, \mathbf{r}) \rangle_H = \frac{1}{4\pi^3 v_F v_g} \frac{1}{\pi R^2} \int_{\varepsilon_0}^R dr r \int_0^{2\pi} d\beta \int_{-\pi/c}^{\pi/c} dk_z \times (|\alpha_1(\mathbf{r})| + |\alpha_2(\mathbf{r})| + |\alpha_3(\mathbf{r})| + |\alpha_4(\mathbf{r})|). \quad (12)$$

This leads to the result

$$\langle N(0, \mathbf{r}) \rangle_H \approx \frac{8}{\pi^3 v_g c} \frac{1}{\pi R} \left[\sqrt{b^2 + C^2} E\left(\frac{b^2}{b^2 + C^2}\right) + \sqrt{b^2 + S^2} E\left(\frac{b^2}{b^2 + S^2}\right) \right] \quad (13)$$

where $b = v'_c / v_F$, c is the lattice constant in the c direction, $C = \cos \epsilon$, $S = \sin \epsilon$ and E is the complete elliptic integral of

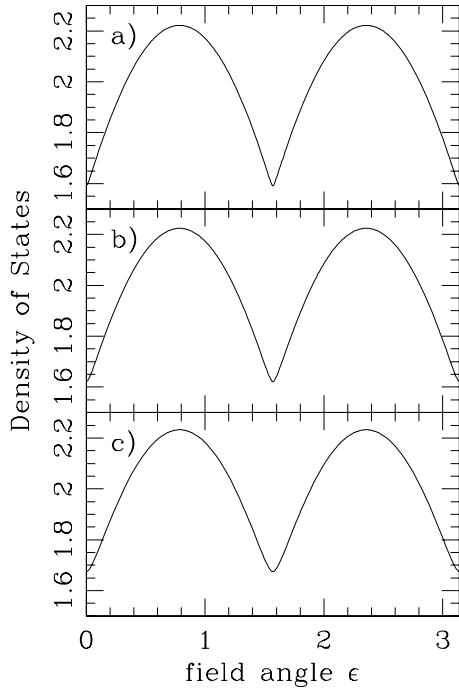


Figure 2. Clean limit density of states (the dimensionless expression in the square brackets of equation (14)) as a function of rotating field angle ϵ (in radians) for $b = 0.02, 0.05$ and 0.10 .

the second kind. Using $N_F \sim 1/cv_g\xi_0$ and $\xi_0/R \sim \sqrt{H/H_{c2}}$, we find

$$\langle N(0, \mathbf{r}) \rangle_H \sim N_F \sqrt{\frac{H}{H_{c2}}} \left[\sqrt{b^2 + C^2} E\left(\frac{b^2}{b^2 + C^2}\right) + \sqrt{b^2 + S^2} E\left(\frac{b^2}{b^2 + S^2}\right) \right]. \quad (14)$$

This function is shown in figure 2 for various values of b . It is seen that deviations from the perfectly 2D cylindrical Fermi surface leads to a softening of the cusps in the density of states. Won and Maki [21] performed a similar calculation of the density of states, and also obtained analytic expressions in terms of elliptic integrals. However, their final results are slightly different due to different considerations; in particular, the cusp features shown in figure 2 do not appear in [21].

In the dirty limit $|\alpha_j/\Gamma_0| \ll 1$ we get

$$\langle N(0, \mathbf{r}) \rangle_H = \frac{\Gamma_0}{4\pi^3 v_F v_g} \frac{1}{\pi R^2} \int_{\xi_0}^R dr r \int_0^{2\pi} d\beta \int_{-\pi/c}^{\pi/c} dk_z \times \left(4 \ln \frac{p_0}{\Gamma_0} + \frac{\alpha_1^2(\mathbf{r})}{\Gamma_0^2} + \frac{\alpha_2^2(\mathbf{r})}{\Gamma_0^2} + \frac{\alpha_3^2(\mathbf{r})}{\Gamma_0^2} + \frac{\alpha_4^2(\mathbf{r})}{\Gamma_0^2} \right) \quad (15)$$

which produces no oscillations with respect to the rotating field.

3. Thermal conductivity

The thermal conductivity tensor is given by the Kubo formula, which is expressed in terms of the imaginary part of Green's function as

$$\frac{\tilde{\kappa}(0, \mathbf{r})}{T} = \frac{k_B^2}{3} \sum_{\mathbf{k}} v_F v_F \text{Tr}[\text{Im} \tilde{G}_{\text{ret}}(0, \mathbf{r}) \text{Im} \tilde{G}_{\text{ret}}(0, \mathbf{r})], \quad (16)$$

where k_B is the Boltzmann constant and v_F is the Fermi velocity in the direction of \mathbf{k} . By again dividing the volume of integration into four regions and introducing the integration variable $p = \sqrt{v_F^2 k_1^2 + v_g^2 k_2^2}$ we find

$$\frac{\tilde{\kappa}(0, \mathbf{r})}{T} = \frac{k_B^2}{3} \frac{1}{(2\pi^3) v_F v_g} \int_0^{2\pi} d\phi \int_0^{p_0} dp p \int_{-\pi/c}^{\pi/c} dk_z \times \sum_{j=1}^4 (v_F v_F)_j \frac{2\Gamma_0^2}{[(\alpha_j(\mathbf{r}) + p)^2 + \Gamma_0^2]^2} \quad (17)$$

$$= \frac{k_B^2}{6\pi^2 v_F v_g} \int_{-\pi/c}^{\pi/c} dk_z \sum_{j=1}^4 (v_F v_F)_j \times \left(1 + \frac{\alpha_j(\mathbf{r})}{\Gamma_0} \left(\tan^{-1} \frac{\alpha_j(\mathbf{r})}{\Gamma_0} - \frac{\pi}{2} \right) \right). \quad (18)$$

Using (2) and (3), in zero magnetic field we get

$$\frac{\tilde{\kappa}(0, 0)}{T} = \frac{2k_B^2 v_F}{3\pi c v_g} \begin{pmatrix} 1 & 0 & 0 \\ 0 & 1 & 0 \\ 0 & 0 & (v_F/v_g)^2 \end{pmatrix}. \quad (19)$$

In a finite magnetic field, terms linear in the Doppler shift will vanish upon integration. So the magnetic part of the thermal conductivity is

$$\frac{\delta \tilde{\kappa}(0, \mathbf{r})}{T} = \frac{k_B^2}{6\pi^2 v_F v_g} \int_{-\pi/c}^{\pi/c} dk_z \sum_{j=1}^4 (v_F v_F)_j \times \frac{\alpha_j(\mathbf{r})}{\Gamma_0} \tan^{-1} \frac{\alpha_j(\mathbf{r})}{\Gamma_0}. \quad (20)$$

In the clean limit, this reduces to

$$\frac{\delta \tilde{\kappa}(0, \mathbf{r})}{T} = \frac{k_B^2}{12\pi v_F v_g} \int_{-\pi/c}^{\pi/c} dk_z \sum_{j=1}^4 (v_F v_F)_j \frac{|\alpha_j(\mathbf{r})|}{\Gamma_0}. \quad (21)$$

The integrand is

$$\frac{v_F^2}{\Gamma_0} \begin{pmatrix} |\alpha_2| + |\alpha_4| & 0 \\ 0 & |\alpha_1| + |\alpha_3| \\ \frac{v_F'}{v_F} (|\alpha_2| - |\alpha_4|) \sin ck_z & \frac{v_F'}{v_F} (|\alpha_1| - |\alpha_3|) \sin ck_z \\ \frac{v_F'}{v_F} (|\alpha_2| - |\alpha_4|) \sin ck_z & \frac{v_F'}{v_F} (|\alpha_1| - |\alpha_3|) \sin ck_z \\ \frac{v_F'}{v_F} (|\alpha_1| + |\alpha_2| + |\alpha_3| + |\alpha_4|) \sin^2 ck_z \end{pmatrix}. \quad (22)$$

The off-diagonal components vanish in the vortex average and the diagonal components are

$$\frac{\langle \delta \kappa_{xx} \rangle_H}{T} = \frac{4}{3\pi^2} \frac{k_B^2}{R\Gamma_0} \frac{v_F^2}{v_g c} \sqrt{b^2 + S^2} E\left(\frac{b^2}{b^2 + S^2}\right) \quad (23)$$

$$\frac{\langle \delta \kappa_{yy} \rangle_H}{T} = \frac{4}{3\pi^2} \frac{k_B^2}{R\Gamma_0} \frac{v_F^2}{v_g c} \sqrt{b^2 + C^2} E\left(\frac{b^2}{b^2 + C^2}\right) \quad (24)$$

$$\frac{\langle \delta \kappa_{zz} \rangle_H}{T} = \frac{4}{9\pi^2} \frac{k_B^2}{R\Gamma_0} \frac{v_F^2}{v_g c} \left(\sqrt{b^2 + S^2} \left[-S^2 K\left(\frac{b^2}{S^2 + b^2}\right) + (2b^2 + S^2) E\left(\frac{b^2}{S^2 + b^2}\right) \right] + \sqrt{b^2 + C^2} \left[-C^2 K\left(\frac{b^2}{C^2 + b^2}\right) + (2b^2 + C^2) E\left(\frac{b^2}{C^2 + b^2}\right) \right] \right) \quad (25)$$

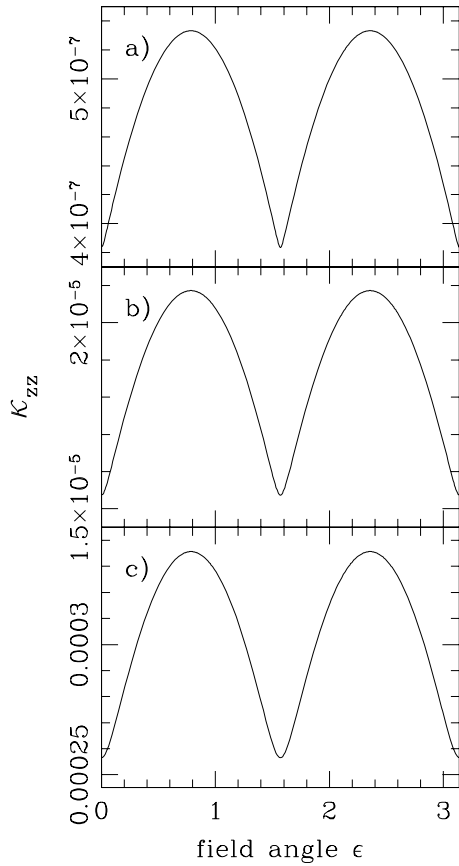


Figure 3. Clean limit thermal conductivity κ_{zz} (the dimensionless expression in the round brackets of equation (25)) as a function of rotating field angle ϵ (in radians) for $b = 0.02, 0.05$ and 0.10 .

where K is the complete elliptic integral of the first kind. κ_{zz} is plotted in figure 3 for different values of b . In the limit $b \rightarrow 0$ the cusps are sharp; however, the oscillation amplitude goes to zero. The oscillation amplitude increases rapidly with b .

In the dirty limit, (20) reduces to

$$\frac{\delta\bar{\kappa}(0, \mathbf{r})}{T} = \frac{k_B^2}{6\pi^2 v_F v_g} \int_{-\pi/c}^{\pi/c} dk_z \sum_{j=1}^4 (\mathbf{v}_F \mathbf{v}_F)_j \frac{\alpha_j^2(\mathbf{r})}{\Gamma_0^2}. \quad (26)$$

Again, the off-diagonal components vanish in the vortex average and the diagonal elements are

$$\left\langle \frac{\delta\kappa_{xx}(0, \mathbf{r})}{T} \right\rangle_H = \frac{k_B^2 v_F^3}{12\pi v_g} \log(R/\xi_0) (2C^2 + b^2) \quad (27)$$

$$\left\langle \frac{\delta\kappa_{yy}(0, \mathbf{r})}{T} \right\rangle_H = \frac{k_B^2 v_F^3}{12\pi v_g} \log(R/\xi_0) (2S^2 + b^2) \quad (28)$$

$$\left\langle \frac{\delta\kappa_{zz}(0, \mathbf{r})}{T} \right\rangle_H = \frac{k_B^2 v_F^3}{12\pi v_g} \log(R/\xi_0) (1 + 3b^2/2). \quad (29)$$

Similar to the dirty limit density of states (15), there are no rotating-field-dependent oscillations in the dirty limit of κ_{zz} .

4. Discussion and conclusions

The topology of the true Fermi surface of $\text{YNi}_2\text{B}_2\text{C}$ shown in [15] is difficult to discern: however, the validity of our

calculation only requires that the Fermi surface exists at the positions of the nodes and spans all or most of the Brillouin zone in the c direction with a slight curvature characterized by the parameter b . The main point is that the cusp features observed in the field angle-dependent heat capacity [10] are a feature of *line nodes* and the cusp features observed in the field angle-dependent thermal conductivity are a feature of *line nodes on a quasi-2D Fermi surface*.

Alternatively, a scenario involving point nodes that vanish quadratically in k , such as that proposed by Maki *et al* [22], will display the same qualitative features as line nodes on a cylindrical Fermi surface. The thermodynamics are the same and a non-zero Fermi velocity in the c direction in the vicinity of the node is required. A semiclassical treatment of quasiparticles originating from quadratic point nodes does not depend on the shape of the Fermi surface outside the vicinity of nodes. While this scenario does satisfactorily account for experimental observations, it must be noted that, among all possible symmetry-allowed order parameters for a superconductor with D_{4h} symmetry, there are none with symmetry-required quadratic point nodes [8, 9].

In the wake of the Maki *et al* proposed gap function, several improvements to the semiclassical (Doppler shift) treatment of point node superconductors have been implemented, all of which include realistic anisotropy of the Fermi velocity in the a - b plane [24–26]. However, as we now show, our semiclassical results are in reasonable *quantitative* agreement with experimental results. Using $R \approx 4 \times 10^{-8}$ m (for a 1 T field), $T = 0.56$ K, $E_F = 9$ Ryd [15], $v_F \approx 3 \times 10^7$ m s $^{-1}$, gap maximum $\Delta_0 = v_g \hbar k_F = 30$ K and scattering rate $\Gamma_0 = 1$ K leads to an estimate of the prefactor in (25) of $\frac{4T}{9\pi^2} \frac{k_B^2}{RT_0} \frac{v_F^2}{v_g c} \approx 10^4$ W K $^{-1}$ m $^{-1}$. The experimentally observed oscillation amplitude is $\approx 2 \times 10^{-3}$ W K $^{-1}$ m $^{-1}$. Comparing with the oscillation amplitudes shown in figure 3, one may deduce that the value of b is approximately 0.02. Such a small value of b produces sharp cusps in the field angle-dependent κ_{zz} oscillations and is therefore fully consistent with experiment.

Finally, we comment on the uniqueness of the proposed order parameter, $\Delta \sim k_x k_y$. As we discussed in section 1, and as shown by our calculations of angle-dependent thermal conductivity, most experiments (with the possible exception of early heat capacity measurements) are best explained by a superconducting gap function with line nodes and not point nodes. Moreover, the angular dependence of the thermal conductivity indicates that the nodes are in the directions $k_x = 0$ and $k_y = 0$. Among all possible superconducting order parameters for a crystal with D_{4h} symmetry classified in [8] and [9], the gap function $\Delta \sim k_x k_y$, which belongs to the irreducible representation B_{2g} of the point group D_{4h} , is the only one with line nodes in the directions $k_x = 0$ and $k_y = 0$ only.

Thus the most straightforward model that best describes accumulated observations on $\text{YNi}_2\text{B}_2\text{C}$ is that the superconducting gap function is $\Delta \sim k_x k_y$, which belongs to the irreducible representation B_{2g} of the point group D_{4h} , with associated line nodes along $k_x = 0$ and $k_y = 0$.

References

- [1] Izawa K, Kamata K, Nakajima Y, Matsuda Y, Watanabe T, Nohara M, Takagi H, Thalmeier P and Maki K 2002 *Phys. Rev. Lett.* **89** 137006
- [2] Cava R J, Takagi H, Zandbergen H W, Krajewski J J, Peck W F Jr, Sigrist T, Batlogg B, van Dover R B, Felder R J, Mizuhashi K, Lee J O, Eisaki H and Uchida S 1994 *Nature* **367** 252
- [3] Godart C, Gupta L C, Nagarajan R, Dhar S K, Noel H, Potel M, Mazumdar C, Hossain Z, Levy-Clement C, Schiffmacher G, Padalia B D and Vijayaraghavan R 1995 *Phys. Rev. B* **51** 489
- [4] Nohara M, Isshiki M, Sakai F and Takagi H 1999 *J. Phys. Soc. Japan* **68** 1078
Nohara M, Suzuki H, Mangkorntong N and Takagi H 2000 *Physica C* **341–348** 2177
- [5] Izawa K, Shibata A, Matsuda Y, Kato Y, Takeya H, Hirata K, van der Beek C J and Konczykowski M 2001 *Phys. Rev. Lett.* **86** 1327
- [6] Zheng G-Q, Wada Y, Hashimoto K, Kitaoka Y, Asayama K, Takeya H and Kadowaki K 1998 *J. Phys. Chem. Solids* **59** 2169
- [7] Yang I-S, Klein M V, Cooper S L, Canfield P C, Cho B K and Lee S-I 2000 *Phys. Rev. B* **62** 1291
- [8] Volovik G E and Gor'kov L P 1985 *Sov. Phys.—JETP* **61** 843
- [9] Sigrist M and Ueda K 1991 *Rev. Mod. Phys.* **63** 239
- [10] Park T, Salamon M B, Choi E M, Kim H J and Lee S-I 2003 *Phys. Rev. Lett.* **90** 177001
- [11] Matsuda Y, Izawa K and Vekhter I 2006 *J. Phys.: Condens. Matter* **18** R705
- [12] Sigrist T 1994 *Nature* **367** 254
- [13] Lee J I, Zhao T S, Kim I G, Min B I and Youn S J 1994 *Phys. Rev. B* **50** 4030
- [14] Singh D J 1996 *Solid State Commun.* **98** 899
- [15] Yamaguchi K, Katayama-Yoshida H, Yanase A and Harima H 2004 *Physica C* **412–414** 225
- [16] Volovik G E 1993 *JETP Lett.* **58** 471
- [17] Aubin H, Behnia K, Ribault M, Gagnon R and Taillefer L 1997 *Phys. Rev. Lett.* **78** 2624
- [18] Vekhter I, Hirschfeld P J, Carbotte J P and Nicol E J 1999 *Phys. Rev. B* **59** R9023
- [19] Izawa K, Yamaguchi H, Matsuda Y, Shishido H, Settai R and Onuki Y 2001 *Phys. Rev. Lett.* **87** 057002
- [20] Abu Alrub T R and Curnoe S H 2008 *Phys. Rev. B* **78** 104521
- [21] Won H and Maki K 2001 *Europhys. Lett.* **56** 729
- [22] Maki K, Thalmeier P and Won H 2002 *Phys. Rev. B* **65** 140502
Thalmeier P and Maki K 2003 *Acta Phys. Pol.* B **34** 557
- [23] Durst A C and Lee P A 2000 *Phys. Rev. B* **62** 1270
- [24] Miranovic P, Ichioka M, Machida K and Nakai N 2005 *J. Phys.: Condens. Matter* **15** 7971
- [25] Udagawa M, Yanase Y and Ogata M 2005 *Phys. Rev. B* **71** 024511
- [26] Nagai Y, Kato Y, Hayashi N, Yamauchi K and Harima H 2007 *Phys. Rev. B* **76** 214514
Nagai Y and Hayashi N 2008 *Phys. Rev. Lett.* **101** 097001
Nagai Y, Hayashi N, Kato Y, Yamauchi K and Harima H 2009 *J. Phys.: Conf. Ser.* **150** 052177